Langmuir

Article

pubs.acs.org/Langmuir

Single-Chain Semiconducting Polymer Dots

Fangmao Ye,[†,§] Wei Sun,[†,§] Yue Zhang,[†] Changfeng Wu,[†,∥] Xuanjun Zhang,[†,⊥] Jiangbo Yu,[†] Yu Rong,[†] Miqin Zhang,[‡] and Daniel T. Chiu*[,†]

[†]Department of Chemistry and [‡]Department of Material Science and Engineering, University of Washington, Seattle, Washington 98195, United States

Supporting Information

ABSTRACT: This work describes the preparation and validation of single-chain semiconducting polymer dots (*s*Pdots), which were generated using a method based on surface immobilization, washing, and cleavage. The *s*Pdots have an ultrasmall size of ∼3.0 nm as determined by atomic force microscopy, a size that is consistent with the anticipated diameter calculated from the molecular weight of the single-chain semiconducting polymer. *s*Pdots should find use in biology and medicine as a new class of fluorescent probes. The FRET assay this work presents is a simple and rapid test to ensure methods developed for preparing *s*Pdot indeed produced single-chain Pdots as designed.

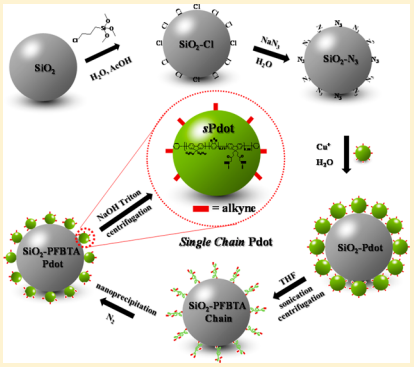

INTRODUCTION

Semiconducting polymer dots (Pdots) have recently emerged as a new class of fluorescent probes that possess large absorption cross-section, high quantum yields, and fast emission rates.[1−10] Pdots have been used for biological detection and imaging,[11−14] biosensing,[15] photoacoustic molecular imaging probes,[16] and specific cellular and subcellular imaging.[6,17]

Pdots that comprise a single polymer chain would cause it to adopt an ultrasmall compact conformation, which would decrease nonspecific binding owing to reduced surface area[18] and also improve its ability to navigate through crowded cellular and subcellular spaces. Despite the advantage of small single-chain Pdots (*s*Pdot), they have not been reported so far. The preparation of *s*Pdot can be difficult using conventional Pdot preparation methods, such as reprecipitation[19] or microemulsion,[20−23] because these methods cause the co-precipitation of multiple chains into one Pdot. Importantly, there is no reliable and simple method to ascertain that potential *s*Pdots produced with a new method indeed are comprised of only a single polymer chain.

With reprecipitation,[19] it is conceivable that one may form *s*Pdots if one starts with an extremely dilute solution of the starting dissolved polymer in tetrahydrofuran (THF) prior to the addition of aqueous solution and the reprecipitation process. The rationale behind this approach is that the polymers are so dilute that they will not encounter each other during polymer chain collapse and thus will form *s*Pdots. In our experiments, however, we found this approach does not work in practice. Table S1 of the Supporting Information shows our results, in which we tested this strategy on three types of polymers poly[(9,9-dioctylfluorenyl-2,7-diyl)-*alt*-*co*-(1,4-benzo-{2,1′,3}-thiadiazole)] (PFBT), poly[(9,9-dioctyl-2,7-divinylene-fluorenylene)-*alt*-*co*-{2-methoxy-5-(2-ethylhexyloxy)-1,4-phenylene}] (PFPV), and poly(9,9-dioctylfluorenyl-2,7-diyl) (PFO). Despite the extremely dilute solution of polymer in THF (0.0005% (w/w)), we were unable to generate Pdots smaller than ∼10 nm with these polymers. At ∼10 nm, each Pdot would comprise multiple chains of polymer, given the molecular weight of the polymers used. There is, however, one report suggesting MEH-PPV [poly(2-methoxy-5-(2′-ethylhexyloxy)-1,4-phenylenevinylene)] polymer with high molecule weight (i.e., M_w > 200,000) may be able to partially form single-chain nanoparticles via the reprecipitation method if a very dilute polymer-in-THF solution (0.005%; 10× higher concentration than our experiments) was used.[24] This result, however, may not be generalized for other semiconducting polymers as indicated by the data shown in Table S1 of the Supporting Information. More importantly, it has been difficult to validate that the Pdots formed with this method indeed comprise only a single polymer chain, because the main evidence was the Pdot size. Yet, the dynamic light scattering and electron microscopy cannot readily identify the diameter difference between Pdots having one and those having two or three polymer chains.

Here, we present a general approach for generating *s*Pdots and also describe a simple fluorescence resonance energy transfer (FRET) assay for validating that the formed Pdots are indeed composed of a single polymer chain. We anticipate this simple assay to be broadly applicable for use in the

Received: October 2, 2014
Revised: December 3, 2014
Published: December 18, 2014

   dx.doi.org/10.1021/la5038684 | *Langmuir* 2015, 31, 499−505

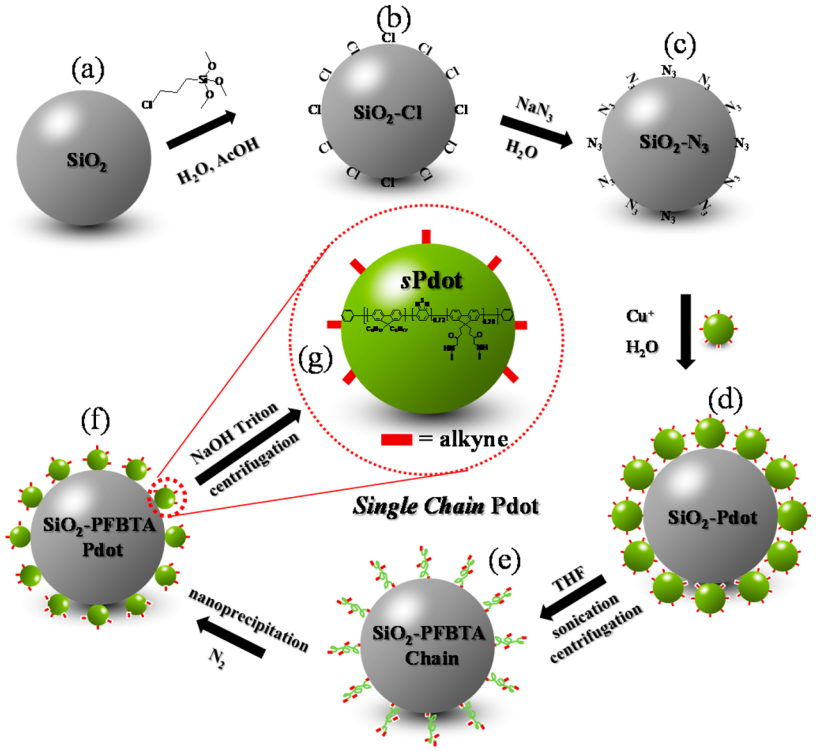

Figure 1. Procedure for preparing single-chain Pdots (*s*Pdots). A silica particle with a diameter of ~200 nm (a) was prepared and the surface modified with a layer of chloride (SiO_2−Cl) (b) via the hydrolysis and condensation of chloridetrimethoxysilane. The SiO_2−Cl groups were then modified to azide to form a clickable silica nanoparticle (c) (Supporting Information). Separately, multichain PFBTA Pdots were prepared using reprecipitation (green spheres); these Pdots had alkyne groups so they could react with the SiO_2−N_3 on the silica surface via click chemistry (d). Once the multichain PFBTA Pdots were clicked onto the surface of the silica nanoparticle, the solvent was changed from aqueous solution to THF and the silica−polymer complex was washed in THF several times (e). This step removed all of the polymer chains in the multichain Pdot and those that were not covalently attached to the silica surface. The single polymer chains attached to the surface of the silica nanoparticles were then reprecipitated into extremely small *s*Pdots by reintroducing the silica−polymer complex to aqueous solution from THF (f). Finally, the PFBTA *s*Pdots were cleaved from the silica surface and released into solution in the presence of NaOH and Triton 100 (g); NaOH hydrolyzed the Si−O bond while Triton 100 prevented the released *s*Pdots from aggregating in the presence of strong base. To remove NaOH and Triton 100, the *s*Pdot solution was dialyzed overnight in water or buffer.

development of various approaches for creating small compact *s*Pdot.

EXPERIMENTAL SECTION

Synthesis of Semiconducting Polymers. The synthesis and structure characterization of alkyne-functionalized PFBTA (poly[(9,9-dioctylfluorenyl-2,7-diyl)-*co*-(1,4-benzo-{2,10,3}-thiadazole)]; M_n = 21,000; polydispersity = 2.1) and alkyne-functionalized PFOA (poly[(9,9-dioctylfluorenyl-2,7-diyl)-*co*-(9,9-dipropylcarboxylfluorenyl-2,7-diyl)]; M_n = 21,000; polydispersity = 2.1) are shown in Figure S1 and Figure S2, respectively, of the Supporting Information.

Preparation of Multichain Pdots. The preparation of multichain Pdots has been described previously.[25] Briefly, 2 mg of the semiconducting polymer, PFBTA or PFOA, was dissolved in 2 mL of THF by stirring overnight in an inert atmosphere. The solution was then filtered through a 0.7 μm glass fiber filter to remove any insoluble material. Multichain Pdots were prepared by injecting 200 μL of 1 mg/mL polymer (in THF) into 10 mL of Milli-Q water under sonication. The THF was removed and the solution concentrated by continuous nitrogen stripping to 10 mL on a 90 °C hot plate. The solution was poured through a 0.2 μm filter.

Preparation of Physically Mixed and Blended Multichain PFOA−PFBTA Pdots. The physically mixed samples with different PFOA/PFBTA ratios were prepared as follows: 40 ppm of multichain PFOA Pdots and 40 ppm of multichain PFBTA Pdots were prepared using the regular reprecipitation method. The sizes of multichain PFOA Pdots and PFBTA Pdots were 13 and 18 nm, respectively, as measured by dynamic light scattering (DLS). The 5%, 10%, 20%, and 50% mixed samples were prepared by adding 50, 100, 200, and 500 μL of 40 ppm multichain PFOA Pdots to 1 mL of 40 ppm multichain PFBTA Pdots, and the samples were noted as 5% M (M for mixed), 10% M, 20% M, and 50% M, respectively. Figure S3 of the Supporting Information shows the absorbance of the preceding samples (top) and the linear dependence of the ratio of absorbance (RA = Abs_{370nm}/Abs_{450nm}) to the ratio of PFOA/ PFBTA (bottom).

The blended multichain PFOA−PFBTA Pdots with different PFOA/PFBTA ratios were prepared as follows: 1000 ppm PFOA polymer in THF and 1000 ppm PFBTA polymer in THF were prepared and filtered through a 0.7 μm glass fiber filter. Then 8, 16, 32, and 80 μL of 1000 ppm PFOA polymer were added to 160 μL of 1000 ppm PFBTA polymer to make 5 mL solutions in THF; the samples were noted as 5% B (B for blended), 10% B, 20% B, and 50% B, respectively. The blended multichain PFOA−PFBTA Pdots were then prepared by injecting the preceding prepared solutions into 10 mL of DI water under sonication. The THF was removed, and the solution was concentrated by continuous nitrogen stripping to 10 mL on a 90 °C hot plate, followed by filtration through a 0.2 μm filter. The absorbance of the blended multichain Pdot

dx.doi.org/10.1021/la5038684 | *Langmuir* 2015, 31, 499−505

samples (not shown) was identical to those of the mixed samples.

Preparation of PFBTA and PFOA–PFBTA *s*Pdot. A 1 mL aliquot of 100 ppm multichain PFBTA Pdots prepared by reprecipitaion from 100 ppm PFBTA in THF (Sigma-Aldrich, dehydrate) solution or 1 mL of blended multichain Pdots prepared by reprecipitaion from 50 ppm PFOA and 100 ppm PFBTA in THF solution was added to 2 mL of 10 mg/mL azide-modified silica particles, SiO_2–N_3, in the presence of freshly prepared $CuSO_4$ (0.5 mM, Sigma-Aldrich, >99%) and L-sodium ascorbate (0.2 mM, Sigma, >98%). The preparation of SiO_2–N_3 was shown in the Supporting Information. The click reaction lasted for 2 h. Then the Pdot–silica particles were centrifuged down and rinsed three times with DI water, after which the solvent was changed to THF and the Pdot–silica was rinsed with THF solution under sonication (5 min). The solution was centrifuged (6000 rpm × 10 min), and the THF rinsing process was repeated three times. A 1 mL aliquot of the resulting Pdot–silica complex in THF solution was then injected into 2 mL of aqueous solution with sonication, and the resulting solution was heated at 80 °C with N_2 stripping for 30 min to remove THF. The final solution (~2 mL) was filtered with 1 μm membrane, and the solvent was changed to aqueous solution containing 100 mM NaOH (Sigma) and 0.25% Triton 100 (Electron Microscopy Science) to cleave the Pdots from the silica surface. The solution was stirred overnight at room temperature, and the Pdots were collected from the supernatant by centrifuging the solution (6000 rpm × 10 min). The pellet after centrifugation was not fluorescent indicating the complete cleavage of Pdots from the silica surface. The supernatant containing Pdots was further dialyzed with DI water to remove the NaOH and Triton 100. The final concentration of the Pdots was ~1 ppm in 2 mL of DI water. The *s*Pdots were stable in several buffers that we tested, including TRIS, TBE, PBS, and HEPES, without showing any size change for up to 6 months of storage at 4 °C.

RESULTS AND DISCUSSION

Generation of *s*Pdots via Surface Immobilization, Washing, and Cleavage. Figure 1 shows the surface immobilization, washing, and cleavage strategy we developed to generate *s*Pdots. Figure 2 shows the structure of the alkyne-functionalized PFBTA and alkyne-functionalized PFOA polymer as well as the optical property and size of their corresponding multichain Pdots. We prepared silica particles with the azide click-functional groups on the surface so that we could bind multichain Pdots onto the surface of a silica particle. To prepare the silica particles, we used the Stöber method[26] and then grafted the silica surface with chloride groups (SiO_2–Cl). The SiO_2–Cl groups were then modified to SiO_2–N_3. To react the PFBTA Pdot–alkyne moieties to the silica–azide groups, we generated Cu^+ in situ from the oxidation–reduction reaction between freshly prepared copper sulfate and L-sodium ascorbate. The multichain PFBTA Pdot was prepared using reprecipitation, and its hydrodynamic diameter of 18 nm is shown in Figure 2d; at this stage, the Pdot bound to the silica surface contained multiple polymer chains. Assuming the silica nanoparticle's surface was fully covered by multichain Pdots, the number of Pdots per silica nanoparticle is ~120, estimated based on the surface area of the silica nanoparticle and the diameter of the multichain Pdots.

To remove the polymer chains in the Pdot that were not bound to the silica surface, we exchanged the solvent from

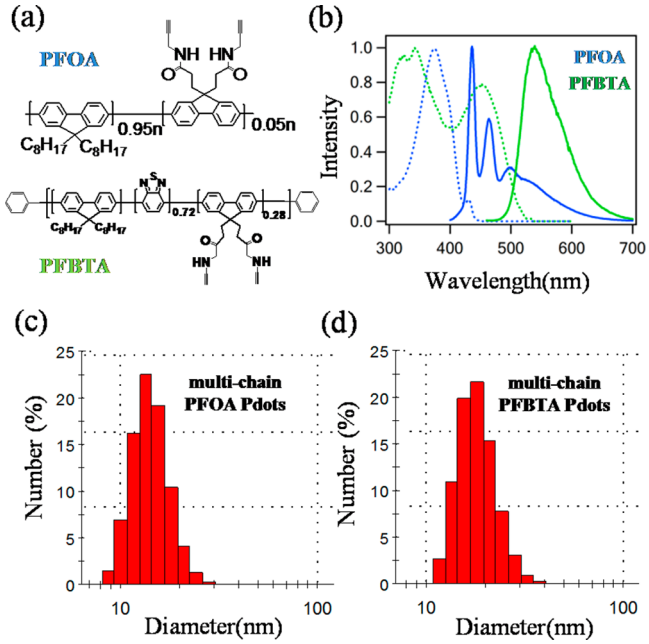

Figure 2. (a) Polymer structure of PFBTA and PFOA. (b) Absorption and emission spectra of multichain PFOA Pdot (blue line) and multichain PFBTA Pdot (green line). Hydrodynamic diameter of (c) the multichain PFOA Pdot and (d) multichain PFBTA Pdot from DLS.

aqueous solution to THF, which solubilized the semiconducting polymers so they were no longer in Pdot form. We washed the silica–polymer complexes with THF multiple times to remove the polymer chains that were not covalently bound to the silica surface through azide–alkyne cycloaddition. After the THF washes, the individual polymer chains attached to the silica surface were rereprecipitated to form single-chain Pdots by returning the silica–polymer particles back to aqueous solution.

After we formed single-chain Pdots that were attached to the silica surface, we cleaved the *s*Pdots from the surface by adding NaOH and Triton 100 to the aqueous solution. NaOH decomposed the Si–O bond, and Triton 100 prevented the cleaved *s*Pdots from aggregating in the presence of NaOH. We performed control experiments (Supporting Information) to show that, for multichain Pdots that did not undergo the THF rinse process, the cleaved Pdots retained the same size and photophysical properties as prior to attachment to the silica surface. Therefore, the attachment of Pdots to the silica surface and the subsequent cleavage to release the Pdots from the surface did not cause any aggregation or damage of the Pdots. This whole process should result in single-chain Pdots (Figure 1).

The key point of this procedure for producing *s*Pdots is to ensure no nonspecific binding between the Pdots and silica surface. The nonspecific binding had been a serious problem in our early experiments, and we had to test many different surface treatments and reaction conditions to address this issue. We finally found that the heat treatment of the silica particles with the surface SiO_2–Cl groups at 70 °C for 24 h resulted in the complete condensation of silanol. This condensation eliminated the nonspecific binding. We carried out several control experiments (Figure S4 of the Supporting Information) to verify that, in the absence of the click reaction, the silica pellet after centrifugation of the Pdot–silica solution was not

dx.doi.org/10.1021/la5038684 | *Langmuir* 2015, 31, 499–505

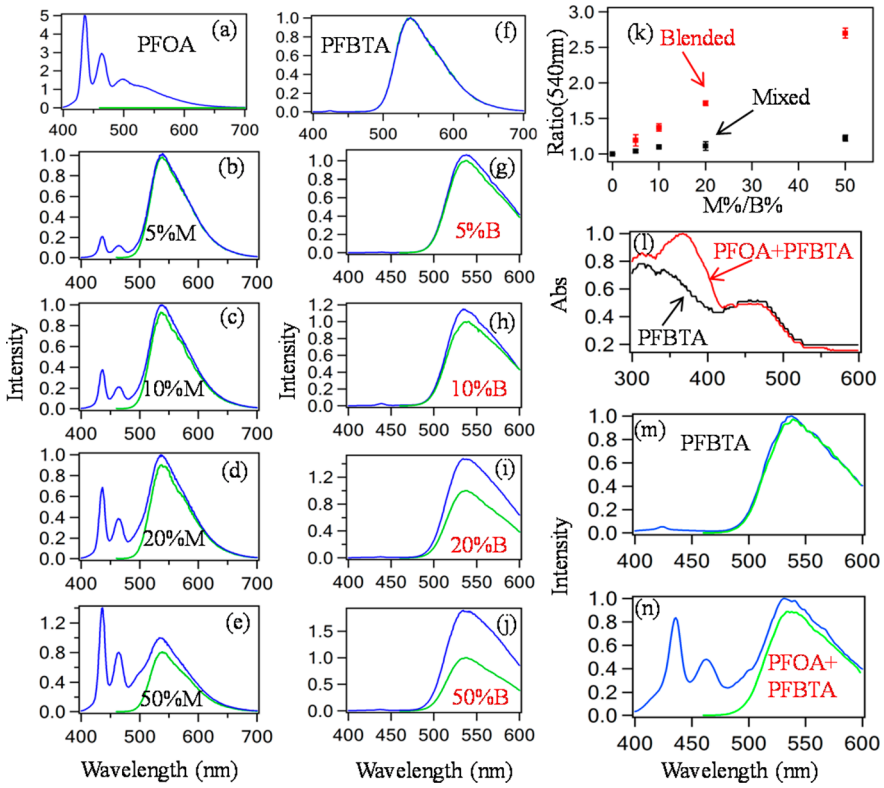

Figure 3. FRET assay for validating that a *s*Pdot was comprised of only a single polymer chain. (a) Fluorescence emission spectra of multichain PFOA Pdot excited at 370 nm (blue) and 450 nm (green). (b–e) Fluorescence emission spectra of different ratios of multichain PFOA Pdots/PFBTA Pdots: (b) 0.05:1 (5% M; M stands for mixed Pdot samples), (c) 0.1:1 (10% M), (d) 0.2:1 (20% M), and (e) 0.5:1 (50% M). (f) Fluorescence emission spectra of multichain PFBTA Pdots excited at 370 nm (blue) and 450 nm (green). (g–j) Fluorescence emission of blended multichain PFOA/PFBTA Pdots at different PFOA/PFBTA blending ratios: (g) 0.05:1 (5% B; B refers to blended Pdot samples), (h) 0.1:1 (10% B), (i) 0.2:1 (20% B), and (j) 0.5:1 (50% B). (k) Plot of the intensity ratio at 540 nm when excited at 370 versus 450 nm (ratio = $I_{\text{excited at 370 nm}}/I_{\text{excited at 450 nm}}$) as a function of PFOA/PFBTA ratios for mixed samples (black square) and blended samples (red square). (l) Absorbance for PFBTA *s*Pdots made from pure multichain PFBTA Pdots (black) and PFOA and PFBTA *s*Pdots made from 50:50 PFOA/PFBTA blended multichain Pdots (red). (m) Fluorescence emission spectra of PFBTA *s*Pdots prepared from multichain PFBTA Pdots when excited at 370 nm (blue) and 450 nm (green). (n) Fluorescence emission spectra of PFOA and PFBTA *s*Pdots prepared from the 50:50 PFOA/PFBTA blended multichain Pdots when excited at 370 nm (blue) and 450 nm (green).

fluorescent so Pdots were not nonspecifically bound to the silica surface. In one control experiment (Figure S4b of the Supporting Information), for example, we omitted copper sulfate in the reaction mixture while keeping all other experimental conditions identical to the procedure for preparing *s*Pdots. We found that the silica pellet was not fluorescent and did not contain any nonspecifically attached polymers.

Validation of Single-Chain Pdots via FRET Assay. To test whether the *s*Pdots that we prepared indeed contained a single polymer chain, we developed a FRET assay. Efficient FRET occurred inside multichain Pdots formed by blending two types of semiconducting polymers.[27] If each Pdot contained two or more polymer chains of different types, the donor polymer's fluorescence would be significantly quenched by the acceptor polymer and the acceptor polymer's fluorescence would be correspondingly enhanced. In contrast, if a Pdot contained only one polymer chain, FRET would not be possible.

We prepared blended multichain Pdots that had two types of alkyne-functionalized semiconducting polymers, PFBTA and PFOA. These two types of polymers showed strong FRET from PFOA to PFBTA when blended into a single Pdot. The blue emission of PFOA was completely absorbed by PFBTA, showing only green PFBTA emission for the blended Pdots. Therefore, if the Pdot contains multiple polymers, such as prior to the THF wash to form single-chain polymers anchored to the silica surface, we should observe strong FRET. However, after *s*Pdots have been formed, FRET should no longer be present. Even if the Pdot contained only two chains of polymer, at a 50% blending ratio, we should still see on average 50% of the Pdots exhibiting FRET. This is because statistically with two polymer chains, we should obtain 25% pure PFOA Pdots, 25% pure FFBTA Pdots, and 50% PFOA–PFBTA Pdots. To experimentally validate this hypothesis, we prepared multichain PFOA–PFBTA Pdots at different blending ratios via reprecipitation.

As a control, we also prepared mixed multichain Pdots, which were pure multichain PFOA and pure multichain PFBTA Pdots mixed together in the same solution at different mixing ratios; here, there should not be FRET because the two types of polymers were in different Pdots.

For the blended multichain PFOA–PFBTA Pdots, we prepared THF solutions with different ratios of PFOA and PFBTA, which resulted in different PFOA/PFBTA ratios inside blended multichain Pdots during reprecipitation. Figure 2 shows the optical properties and size of pure multichain PFOA and PFBTA Pdots. For blended multichain PFOA–PFBTA

dx.doi.org/10.1021/la5038684 | *Langmuir* 2015, 31, 499–505

Pdots, we found the emission of PFOA was completely quenched by PFBTA if the ratio of PFOA/PFBTA in the Pdot was less than 1:2. We measured the lifetime of PFBTA in the blended Pdots, which was ∼0.9 ns, consistent with the result reported elsewhere.[5,6,19] The lifetime of PFOA in the blended Pdots was too short to measure, which is expected given the highly efficient and complete energy transfer to PFBTA. For this reason, we restricted the amount of PFOA to this ratio of 1:2 or less.

Parts a and f of Figure 3 show the emission spectra of pure multichain PFOA Pdots and PFBTA Pdots excited at 370 nm (blue line) and 450 nm (green line). As anticipated, no emission was observed from multichain PFOA Pdots with the 450 nm excitation because of the absence of absorption by PFOA at this wavelength. On the other hand, multichain PFBTA Pdots showed identical emission spectra whether excited at 370 or 450 nm. Although the absorption cross-section of PFBTA at 370 nm is slightly smaller than that at 450 nm (Abs_{450nm}/Abs_{370nm} = 1.09 for PFBTA; Figure 2), the power output of the xenon lamp in the spectrometer (Fluorolog-3) was slightly higher at 370 nm (power output of 370 nm/450 nm = 1.10; Figure S5 of the Supporting Information). It turned out these two factors completely canceled out each other's effects to result in the same emissions for PFBTA regardless of whether 370 or 450 nm excitation was used.

Parts b–e of Figure 3 show the emission spectra of mixed multichain PFOA– and PFBTA–Pdot samples excited at 370 nm (blue line) and 450 nm (green line) at different mixing ratios of PFOA–Pdots/PFBTA–Pdots. Their corresponding absorption spectra are shown in Figure S3 of the Supporting Information. The absolute intensity at 540 nm was mostly from PFBTA Pdots; there was a small contribution from PFOA Pdots due to its broad fluorescence emission (Figure 3a). The small contribution from PFOA Pdots to the 540 nm emission intensity are dependent on the amount of PFOA Pdots in the mixed sample, which were 2.9% for 5% M (Figure 3b), 5.7% for 10% M (Figure 3c), 11.5% for 20% M (Figure 3d), and 18.7% for 50% M (Figure 3e), where M stands for mixed pure multichain Pdot samples. This mixed Pdot sample is different from the blended Pdot sample that we will discuss later; in the blended sample, the two types of polymers are blended together in the *same* Pdot. This was expected because the amount of PFBTA Pdots did not change and there was no FRET between pure multichain PFOA Pdots and pure multichain PFBTA Pdots. Therefore, the small amount of emission at 540 nm from PFOA Pdots gradually increased relative to that of PFBTA Pdots as the amount of PFOA Pdots present in solution increased from 5% M to 50% M.

Parts g–j of Figure 3 show the emission spectra of the blended multichain Pdot samples excited at 370 nm (blue line) and 450 nm (green line) with different PFOA/PFBTA blending ratios. Their corresponding absorption spectra are shown in Figure S3 of the Supporting Information. Compared to the mixed pure multichain Pdot samples, it is clear that the PFOA emission was completely quenched by PFBTA in these blended Pdots. By comparing the emission at 540 nm when excited at 370 or 450 nm, a clear enhancement of 540 nm emission was seen with 370 nm excitation, because in addition to direct excitation of PFBTA, there was the added intensity caused by FRET from PFOA to PFBTA.

Figure 3k shows the relationship between the emission ratio (ratio = $I_{370excited}/I_{450excited}$) at 540 nm and the PFOA/PFBTA ratio for both mixed and blended multichain Pdot samples. For the mixed sample, the emission ratio increased slowly when the PFOA/PFBTA ratio increased, resulting in a ∼23% enhancement at 540 nm for the 1:2 ratio of PFOA/PFBTA. This enhancement is consistent with the broad emission of PFOA, which has a long tail that extends to 540 nm; the emission at 540 nm from PFBTA itself remained the same. In contrast, for the blended sample, the emission ratio increased dramatically, resulting in a 170% enhancement at 540 nm for the 1:2 ratio (50% B, where B stands for blended multichain Pdot samples) of PFOA/PFBTA.

To test if a *s*Pdot contained a single polymer chain, we prepared two *s*Pdot samples, one made from a PFBTA Pdot and the other from a 50% B PFOA/PFBTA blended Pdot. Figure 3m is the control experiment, which shows the emission spectra of PFTBA *s*Pdots made from pure PFTBA Pdots. As expected, the emission at 540 nm was identical regardless of whether the *s*Pdot was excited at 370 or 450 nm because PFOA was not present and there was no FRET. Figure 3n shows the emission spectra of the *s*Pdot solution made from the 50% B PFOA/PFBTA blended Pdots. Similar to the information provided in the absorption spectra (Figure 3l), we observed the presence of PFOA *s*Pdots. Using the calibration curve shown in Figure S3 of the Supporting Information, we calculated the value of PFOA/PFBTA to be ∼0.45, which is consistent with the initial feeding ratio of ∼0.5 that we used to form the blended Pdots. If we looked closer at the 540 nm emission peak, we saw there was only 17% enhancement of the 540 nm peak when the sample was excited at 370 nm versus 450 nm. This 17% enhancement at 540 nm was completely accounted for by the broad emission of PFOA for a PFOA/PFBTA value of 0.45. This observation confirmed the complete absence of FRET and that PFOA was not associated with PFBTA *s*Pdots, even though the initial Pdots used to prepare the *s*Pdots contained a ∼ 1:2 blend of PFOA/PFBTA. This result thus indicates that PFBTA *s*Pdots were indeed comprised of a single chain of PFBTA and that PFOA, which was initially blended into the multichain PFBTA Pdot, was now absent from the single-chain PFBTA *s*Pdot.

Size of Single-Chain Pdots from AFM. The molecular weight of PFBTA was 21,000 g/mol. If we assume that a single chain of PFBTA was fully condensed into a spherical compact dot with a density of ∼1.0 g/cm^3, the resulting single-chain Pdot would have a diameter of ∼3.3 nm. Indeed, the topographic AFM image of *s*Pdots (Figure 4) shows discrete polymer nanoparticles with an average size of about 2.8 nm. It should be noted that differences between the apparent particle width and height were observed in the particle height profiles. This difference is due to the AFM tip's lateral smearing of the

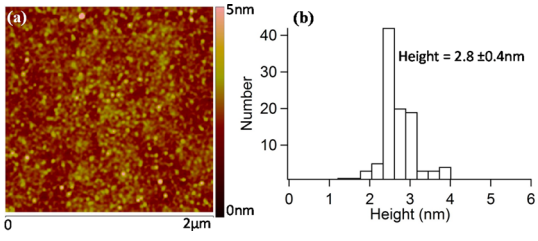

Figure 4. (a) AFM image and (b) its corresponding height histogram of PFBTA *s*Pdots showing a mean particle size of 2.8 ± 0.4 nm (calculated from 100 *s*Pdots). The scale bar in panel a represents 0–5 nm.

dx.doi.org/10.1021/la5038684 | *Langmuir* 2015, 31, 499–505

nanoparticle as well as the convolution of the width of the AFM tip with the width of the particle, and thus the size of the Pdots was determined with the estimated height rather than the lateral width in the AFM images. This 2.8 nm diameter of *s*Pdots from AFM is consistent with the aforementioned calculated size of 3.3 nm, which is consistent with the PFBTA *s*Pdot only containing a single polymer chain.

CONCLUSION

In summary, we have developed a method for producing single-chain Pdots based on surface immobilization, washing, and cleavage. The *s*Pdot formed had a diameter of ∼3 nm, consistent with the expected diameter based on estimations using the molecular weight of a single polymer chain. To verify that each *s*Pdot indeed contained a single chain of polymer, we have developed a simple FRET assay. We anticipate this assay to be useful in the development of *s*Pdots or other fluorescent single-chain polymer nanoparticles.

ASSOCIATED CONTENT

Supporting Information

Text describing additonal information about the experiment and characterizations, table listing sizes of Pdots, and figures showing synthesis routes, absorbance plot, RA dependence as a function of PFOA/PFBTA, control experiments, and xenon lamp intensity profile as a function of wavelength. This material is available free of charge via the Internet at http://pubs.acs.org.

AUTHOR INFORMATION

Corresponding Author

*E-mail: chiu@chem.washington.edu.

Present Addresses

[‖]State Key Laboratory on Integrated Optoelectronics, College of Electronic Science and Engineering, Jilin University, Changchun, Jilin 130012, China.

[⊥]Division of Molecular Surface Physics & Nanoscience, Department of Physics, Chemistry, and Biology, Linköping University, Linköping 58183, Sweden.

Author Contributions

[§]F.Y. and W.S. contributed equally to this work.

Notes

The authors declare the following competing financial interest(s): J.Y., C.W., and D.T.C. have financial interest in Lamprogen, which has licensed the described technology from the University of Washington..

ACKNOWLEDGMENTS

We gratefully acknowledge support of this work by NIH (Grants R21CA186798 and R01NS052637) and the University of Washington.

REFERENCES

(1) Li, K.; Ding, D.; Huo, D.; Pu, K.-Y.; Thao, N. N. P.; Hu, Y.; Li, Z.; Liu, B. Conjugated Polymer Based Nanoparticles as Dual-Modal Probes for Targeted in Vivo Fluorescence and Magnetic Resonance Imaging. *Adv. Funct. Mater.* **2012**, *22*, 3107−3115.

(2) Rahim, N. A. A.; McDaniel, W.; Bardon, K.; Srinivasan, S.; Vickerman, V.; So, P. T. C.; Moon, J. H. Conjugated Polymer Nanoparticles for Two-Photon Imaging of Endothelial Cells in a Tissue Model. *Adv. Mater.* **2009**, *21*, 3492−3496.

(3) Zhu, C.; Liu, L.; Yang, Q.; Lv, F.; Wang, S. Water-Soluble Conjugated Polymers for Imaging, Diagnosis, and Therapy. *Chem. Rev.* **2012**, *112*, 4687−4735.

(4) Pu, K. Y.; Li, K.; Shi, J. B.; Liu, B. Fluorescent Single-Molecular Core-Shell Nanospheres of Hyperbranched Conjugated Polyelectrolyte for Live-Cell Imaging. *Chem. Mater.* **2009**, *21*, 3816−3822.

(5) Das, S.; Powe, A. M.; Baker, G. A.; Valle, B.; El-Zahab, B.; Sintim, H. O.; Lowry, M.; Fakayode, S. O.; McCarroll, M. E.; Patonay, G.; Li, M.; Strongin, R. M.; Geng, M. L.; Warner, I. M. Molecular Fluorescence, Phosphorescence, and Chemiluminescence Spectrometry. *Anal. Chem.* **2012**, *84*, 597−625.

(6) Wu, C.; Jin, Y.; Schneider, T.; Burnham, D. R.; Smith, P. B.; Chiu, D. T. Ultrabright and Bioorthogonal Labeling of Cellular Targets Using Semiconducting Polymer Dots and Click Chemistry. *Angew. Chem., Int. Ed.* **2010**, *49*, 9436−9440.

(7) Pecher, J.; Mecking, S. Nanoparticles of Conjugated Polymers. *Chem. Rev.* **2010**, *110*, 6260−6279.

(8) Abbel, R.; van der Weegen, R.; Meijer, E. W.; Schenning, A. P. H. J. Multicolour self-assembled particles of fluorene-based bolaamphiphiles. *Chem. Commun. (Cambridge, U. K.)* **2009**, 1697−1699.

(9) Pecher, J.; Mecking, S. Nanoparticles from Step-Growth Coordination Polymerization. *Macromolecules* **2007**, *40*, 7733−7735.

(10) Cordovilla, C.; Swager, T. M. Strain Release in Organic Photonic Nanoparticles for Protease Sensing. *J. Am. Chem. Soc.* **2012**, *134*, 6932−6935.

(11) Li, K.; Liu, B. Polymer encapsulated conjugated polymer nanoparticles for fluorescence bioimaging. *J. Mater. Chem.* **2012**, *22*, 1257−1264.

(12) Moon, J. H.; MacLean, P.; McDaniel, W.; Hancock, L. F. Conjugated polymer nanoparticles for biochemical protein kinase assay. *Chem. Commun.(Cambridge, U. K.)* **2007**, 4910−4912.

(13) Hong, G.; Zou, Y.; Antaris, A. L.; Diao, S.; Wu, D.; Cheng, K.; Zhang, X.; Chen, C.; Liu, B.; He, Y.; Wu, J. Z.; Yuan, J.; Zhang, B.; Tao, Z.; Fukunaga, C.; Dai, H. Ultrafast fluorescence imaging in vivo with conjugated polymer fluorophores in the second near-infrared window. *Nat. Commun.* **2014**, DOI: 10.1038/ncomms5206.

(14) Moon, J. H.; McDaniel, W.; MacLean, P.; Hancock, L. F. Live-Cell-Permeable Poly(p-phenylene ethynylene). *Angew. Chem.* **2007**, *119*, 8371−8373.

(15) Ye, F.; Wu, C.; Jin, Y.; Chan, Y.-H.; Zhang, X.; Chiu, D. T. Ratiometric Temperature Sensing with Semiconducting Polymer Dots. *J. Am. Chem. Soc.* **2011**, *133*, 8146−8149.

(16) Pu, K.; Shuhendler, A. J.; Jokerst, J. V.; Mei, J.; Gambhir, S. S.; Bao, Z.; Rao, J. Semiconducting polymer nanoparticles as photoacoustic molecular imaging probes in living mice. *Nat. Nanotechnol.* **2014**, *9*, 233−239.

(17) Pu, K.-Y.; Li, K.; Liu, B. Multicolor Conjugate Polyelectrolyte/Peptide Complexes as Self-Assembled Nanoparticles for Receptor-Targeted Cellular Imaging. *Chem. Mater.* **2010**, *22*, 6736−6741.

(18) Zhang, X.; Yu, J.; Wu, C.; Jin, Y.; Rong, Y.; Ye, F.; Chiu, D. T. Importance of Having Low-Density Functional Groups for Generating High-Performance Semiconducting Polymer Dots. *ACS Nano* **2012**, *6*, 5429−5439.

(19) Wu, C.; Peng, H.; Jiang, Y.; McNeill, J. Energy Transfer Mediated Fluorescence from Blended Conjugated Polymer Nanoparticles. *J. Phys. Chem. B* **2006**, *110*, 14148−14154.

(20) Kietzke, T.; Neher, D.; Landfester, K.; Montenegro, R.; Guntner, R.; Scherf, U. Novel approaches to polymer blends based on polymer nanoparticles. *Nat. Mater.* **2003**, *2*, 408−412.

(21) Landfester, K.; Montenegro, R.; Scherf, U.; Güntner, R.; Asawapirom, U.; Patil, S.; Neher, D.; Kietzke, T. Semiconducting Polymer Nanospheres in Aqueous Dispersion Prepared by a Miniemulsion Process. *Adv. Mater.* **2002**, *14*, 651−655.

(22) Baier, M. C.; Huber, J.; Mecking, S. Fluorescent Conjugated Polymer Nanoparticles by Polymerization in Miniemulsion. *J. Am. Chem. Soc.* **2009**, *131*, 14267−14273.

(23) Lim, J.; Swager, T. M. Fluorous Biphase Synthesis of a Poly(p-phenyleneethynylene) and its Fluorescent Aqueous Fluorous-Phase Emulsion. *Angew. Chem., Int. Ed.* **2010**, *49*, 7486−7488.

(24) Szymanski, C.; Wu, C.; Hooper, J.; Salazar, M. A.; Perdomo, A.; Dukes, A.; McNeill, J. Single Molecule Nanoparticles of the Conjugated Polymer MEHPPV, Preparation and Characterization by

Near-Field Scanning Optical Microscopy. *J. Phys. Chem. B* **2005**, *109*, 8543−8546.
(25) Wu, C.; Schneider, T.; Zeigler, M.; Yu, J.; Schiro, P. G.; Burnham, D. R.; McNeill, J. D.; Chiu, D. T. Bioconjugation of Ultrabright Semiconducting Polymer Dots for Specific Cellular Targeting. *J. Am. Chem. Soc.* **2010**, *132*, 15410−15417.
(26) Stöber, W.; Fink, A.; Bohn, E. Controlled growth of monodisperse silica spheres in the micron size range. *J. Colloid Interface Sci.* **1968**, *26*, 62−69.
(27) Wu, C.; Hansen, S. J.; Hou, Q.; Yu, J.; Zeigler, M.; Jin, Y.; Burnham, D. R.; McNeill, J. D.; Olson, J. M.; Chiu, D. T. Design of Highly Emissive Polymer Dot Bioconjugates for In Vivo Tumor Targeting. *Angew. Chem., Int. Ed.* **2010**, *50*, 3430−3434.